Research article

MRC

Received: 28 January 2015 Revised: 20 March 2015 Accepted: 27 March 2015 Published online in Wiley Online Library: 20 July 2015

(wileyonlinelibrary.com) DOI 10.1002/mrc.4251

Dynamic NMR study of dinitrophenyl derivatives of seven-membered cyclic ketals of pyridoxine

Ilfat Z. Rakhmatullin, Leisan F. Galiullina, Marsel' R. Garipov, Alexey D. Strel'nik, Yurii G. Shtyrlin and Vladimir V. Klochkov*

Two pyridoxine derivatives containing a dinitrophenyl moiety were investigated by ^{1}H NMR spectroscopy. Conformational dynamics in solution were studied for each compound using dynamic NMR experiments. It was shown that both compounds studied are involved into two conformational exchange processes. The first process is a transformation of the seven-membered cycle conformation between the enantiomeric *P*-twist and *M*-twist forms, and the second is a rotation of the dinitrophenyl fragment of the molecules around the C–O bond. Energy barriers of both conformational transitions were determined. Copyright © 2015 John Wiley & Sons, Ltd.

Keywords: dynamic ^{1}H NMR; conformational exchange; energy barrier; pyridoxine; ketal

Introduction

Synthesis of molecular systems with desirable biochemical or physical properties often requires the knowledge of the spatial structure of compounds and the information about their conformational mobility.[1,2] Nowadays, NMR techniques are a powerful tool for conformational analysis of biologically important samples such as pyridoxine derivatives studied here.[3,4]

It is well known that seven-membered cyclic acetals and ketals with planar fragments exist in solution in the dynamic equilibrium of two forms: the chair and the twist.[1,2,5] Previous studies revealed some correlation between steric structure and reactivity of these compounds.[5–8] Recently, we have investigated the conformational transformations of pyridoxine derivatives containing a seven-membered acetal ring with a 2,4-dinitrophenyloxy ortho-substituent[9] revealing properties of organic nonlinear optical materials.[10] In this paper, we present the results of dynamic NMR study of 9-(2,4-dinitrophenyloxy)-3,3,8-trimethyl-1,5-dihydro-[1,3]dioxepino[5,6-c]pyridine and 9-(2,4-dinitrophenyloxy)-3,8-dimethyl-3-pentyl-1,5-dihydro-[1,3]dioxepino[5,6-c]pyridine. Both molecules contain the same ortho-2,4-dinitrophenyloxy substituent, but the substituents at the ketal carbon atom are different. Such molecular configuration leads to significant differences in the conformational transformation of seven-membered rings and provides a good opportunity to study the influence of the rotation around the pyridine–oxygen bond on the conformation of the ketal ring. The distinction of the seven-membered ketals derivatives from previously studied compounds is that there is no chair form[11] of the cycle in solution. The ketal cycle is involved in a rapid conformational exchange between two twist forms at ambient temperature.

Thus, the investigated compounds represent cyclic molecules with several types of intramolecular motions at room temperature. This complicates studying conformational features of the molecules and therefore prediction and explanation of their biochemical and physical properties. NMR experiments with decreasing temperature reveal a slowdown of the conformational exchange rate and thus provide information about the spatial structure of the molecules in solution. This method is also used for calculations of energy parameters of conformational transitions.

Experimental

All NMR experiments were performed on a Bruker Avance II-500 NMR spectrometer (Bruker Biospin AG, Fallanden, Switzerland) equipped with a 5-mm probe using standard Bruker TOPSPIN software (Bruker Corporation). The ^{1}H NMR data were collected with 32 k complex data points and were apodized with a Gaussian window function (lb = −0.5 and gb = 0.2) prior to Fourier transformation. ^{1}H NMR spectra were recorded using 900 pulses, a delay between pulses of 2 s, a spectrum width of 10 ppm, and a minimum of eight scans. Signal-to-noise enhancement was achieved by multiplication of the FID with an exponential window function (lb = 0.5 Hz). The accuracy of the ^{1}H NMR chemical shifts was at least 0.02 ppm, and the accuracy of the spin–spin interaction constant was at least 0.5 Hz.

The assignments of the ^{1}H and ^{13}C NMR signals were achieved from the signal multiplicities, the integral values, and the characteristic chemical shifts from through-bond correlations in the two-dimensional (2D) correlated spectroscopy (COSY) spectra, through-space correlations in the 2D nuclear Overhauser enhancement spectroscopy (NOESY) spectra, and from the ^{1}H–^{13}C heteronuclear correlations in the 2D heteronuclear single-quantum correlation (HSQC) and heteronuclear multiple-bond correlation (HMBC) spectra.

* *Correspondence to: Vladimir V. Klochkov, Kazan (Volga Region) Federal University, 18 Kremlevskaya St, Kazan 420008, Russia. E-mail: vladimir.klochkov@kpfu.ru*

Kazan (Volga Region) Federal University, 18 Kremlevskaya St, Kazan 420008, Russia

All 2D experiments were performed with 2 k × 512 data points; the number of transients (2–16 scans) and the sweep widths were optimized individually. In the homonuclear ^{1}H–^{1}H COSY (Bruker pulse program cosygpqf) and NOESY (noesygpph) experiments, the relaxation delay was set to 2 s and the 90° pulse length to 10.4 μs. The resulting FIDs were zero filled to a 2 × 1 k data matrix and apodized with a sine function for COSY and a shifted sine function for NOESY in both the ω_1 and ω_2 dimensions prior to Fourier transformation. Two-dimensional NOESY experiments were performed with pulsed filtered gradient techniques. The mixing time was 0.15 s. Heteronuclear spectra were recorded with 2 k × 512 data points, zero filled in F1 to a 2 k × 512 data matrix, and apodized in both dimensions with a shifted sine function. HSQC experiments (hsqcetgpsp) were acquired using adiabatic pulses for inversion of ^{13}C and GARP sequence for broadband ^{13}C decoupling and optimized for $^{1}J(CH) = 145$ Hz. The 90° ^{13}C pulse length was 7.5 μs. ^{1}H–^{13}C long-range HMBC spectra (hmbcgplpndqf) were performed with $^{n}J(CH)$ set to 8 Hz.

The dynamic ^{1}H NMR spectra were recorded at different temperatures over the range of 183–303 K every 5 K. Temperature control was achieved using a Bruker variable temperature unit (BVT-2000) in combination with a Bruker cooling unit (BCU-05). The sample was cooled by a flow of low-temperature nitrogen gas from a Dewar with liquid nitrogen. The experiments were performed without sample spinning.

The synthesis of the studied compounds was described in the patent.[12] The NMR samples were prepared by dissolving in solvents: the mixture of $CS_2/CDCl_3$ (9 : 1) and acetone-d_6. Purity of solvents was monitored by ^{1}H NMR spectra. Chemical shifts were given in values of ppm, referenced to a residual solvent signals [2.07 for ^{1}H, 30.5 and 205.1 for ^{13}C in acetone-d_6; 7.26 for ^{1}H, 77.2 for ^{13}C in $CS_2/CDCl_3$ (9 : 1)]. All samples were prepared in standard 5-mm ampoules. The working concentrations of the substances were 0.5% by weight, the solution volume was 0.6 ml, and the stabilizing magnetic field was carried by the deuterium signals of the solvent. For the full line shape analysis, the WinDNMR-Pro 7.1.14 program designed by Hans J. Reich at the University of Wisconsin was used.[13] As an input to the program, the chemical shifts, the transverse relaxation times T_2*, and the constants of the spin–spin interaction were used. Calculation of a rate constant (k) was performed by full line shape analysis using the following expressions:

$$P1\ (k_{ab}) = P_2\ (k_{ba})\ ;\ P_1 + P_2 = 1$$

where P_1 and P_2 represent the populations of the relevant conformers A and B in the resulting NMR signal.

The activation parameters were calculated using the Eyring equation. The errors in the determination of the $\Delta H^{\neq}$ and $\Delta G^{\neq}$ activation parameters were less than 4 and 1 kJ/mol, respectively.[14,15]

The free energy of activation of first-order monomolecular reversible reactions, which include intramolecular rotation processes and interconversions of cyclic systems, can be found using the following equations:[16–18]

$$A \underset{k_{ba}}{\overset{k_{ab}}{\rightleftharpoons}} B$$

$$\Delta G^{\neq} = \Delta H^{\neq} - T\Delta S^{\neq}$$

$$\ln(k/T) = -\Delta H^{\neq}/RT + \Delta S^{\neq}/R + 23.76$$

where $\Delta H^{\neq}$ and $\Delta S^{\neq}$ correspond to the activation enthalpy and entropy, respectively, T is the temperature in K, and R is the universal gas constant.

The calculation of the activation parameters for the coalescence temperature was conducted according to the following equation:[19]

$$\Delta G^{\neq} = 4,57{*}T{*}\left(10,32 + \log_{10}\frac{T}{k}\right)$$

where k is $k = \pi\ ((\Delta\nu^0_{AB})^2 + 6\,J^2)/2^{1/2}$ or in the case of two non-interacting spins (J = 0), $k = \pi\ \Delta\nu^0/1.414$.

For data processing, the Origin Pro 7.5 program (OriginLab Corporation, Northampton, MA, USA) was also used.[20]

Results and discussion

Dynamic ^{1}H NMR study of 9-(2,4-dinitrophenyloxy)-3,3,8-trimethyl-1,5-dihydro-[1,3]dioxepino[5,6-c]pyridine

The molecular structures of the compounds are shown in Fig. 1. Numbering of methyl groups (CH_3-8) in compound I was set equal for convenience because they give one resonance signal in the ^{1}H NMR spectrum at high temperatures (Fig. 1).

To confirm the chemical structure of compound I, one-dimensional ^{1}H and ^{13}C and 2D NMR experiments were carried out. Assignment of the signals in the ^{1}H NMR spectrum (Fig. 2) was made on the basis of 2D COSY, 2D TOCSY, and 2D NOESY spectra (Fig. 2).

The chemical shifts of observed ^{1}H NMR signals at different temperatures are shown in Table 1. Methylene groups CH_2-4 and CH_2-7 have broadened signals in the spectrum at room temperature. These groups presumably participate in partially slowed conformational exchange process in the NMR time scale even at room temperature (Table 1).

In order to obtain the energy characteristics of this process and to determine the conformational structure of the molecule, experiments with decreasing temperature were carried out.

Line shapes of the signals in the ^{1}H NMR spectrum of compound I changed with decreasing temperature (Fig. 2a). At $T = 183$ K, CH_2-4 and CH_2-7 signals transformed into four AB quadruplets. Proton signals CH-20 and CH_3-13 were observed as a pair of doublets and a pair of singlets, respectively, in the spectrum at low temperature. Thus, the number of these signals had been doubled compared with the spectrum at room temperature. The integral intensity of the signals belonging to different forms allowed us to determine the content ratio of the different conformations, which was approximately 1 : 1.65.

To define the energy parameters of conformational transitions, line shape simulation of the NMR spectra at different temperatures

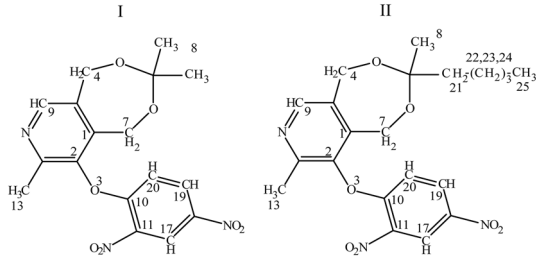

Figure 1. Molecular structures of studied compounds.

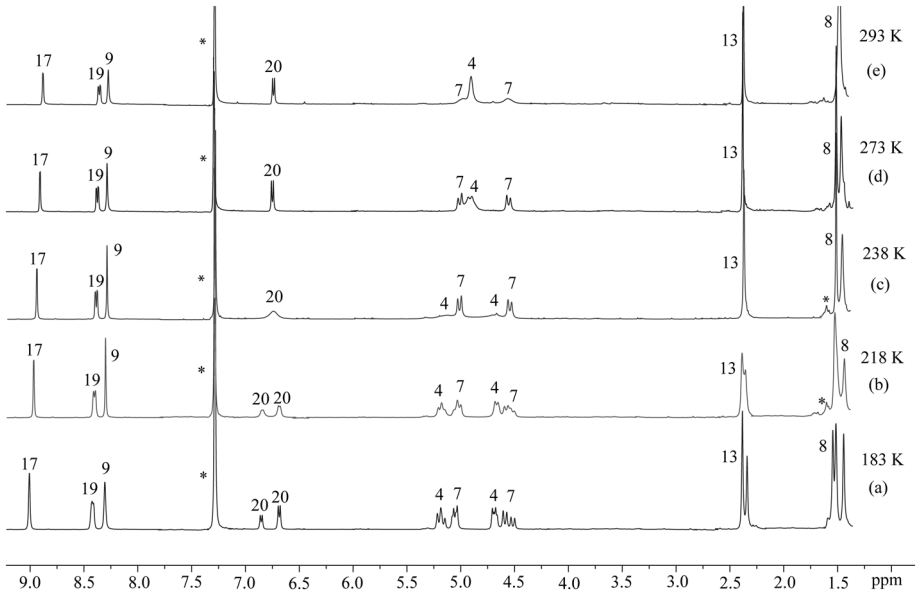

Figure 2. ^{1}H NMR spectra of compound I in $CS_2 + CDCl_3$ (9/1) at different temperatures. The signals of the solvent and impurities are marked by asterisks.

Table 1. ^{1}H NMR spectra parameters (δ, ppm) and spin–spin interaction constants (J, Hz) for compound I in $CS_2/CDCl_3$ (9 : 1) at different temperatures [a]

T, *K*	CH-9	CH_2-4	CH_2-7	CH_3-8	CH_3-13	CH-20	CH-19	CH-17
293	8.29	4.91	4.57*, 4.99*	1.48	2.38	6.74 (9.1)	8.36 (2.1)	8.88 (2.0)
273	8.29	4.91 (17.0)	4.55, 5.00 (16.8)	1.52*, 1.47*	2.38	6.75 (9.1)	8.37 (2.2)	8.90 (2.1)
238	8.31	4.69*, 5.14*	4.55, 5.02 (16.3)	1.52, 1.47*	2.38	6.75*	8.40 (2.1)	8.95 (2.1)
218	8.32	4.67, 5.18 (13.3)	4.55, 5.03 (16.7)	1.53*, 1.44*	2.39*, 2.36*	6.69, 6.85 (7.3)	8.4	8.97 (1.9)
183	8.32*	4.69, 5.19 (15.2)	4.55, 5.05 (17.3)	1.44, 1.52, 1.54	2.39 2.34	6.69, 6.85 (9.0)	8.4	9.01

[a]Notation: chemical shifts of dominant form signals are underlined.
* This means broadened signal.

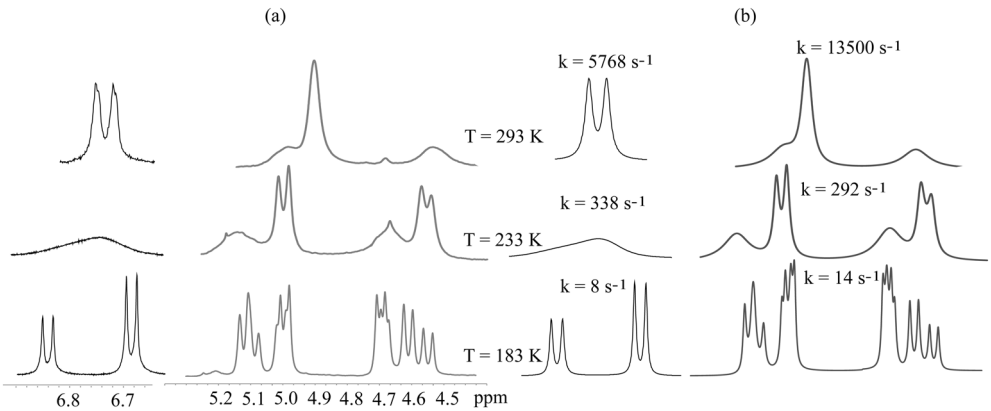

Figure 3. Line shape simulation for the signals CH-20, CH_2-4,7, and corresponding rate constants at different temperatures: (a) experiment and (b) simulation.

was performed. Line shape analysis of the signals CH-20 and CH_2-4,7 at various temperatures was carried out using the program WINDNMR-Pro (Fig. 3).[13] As a result, the temperature dependencies of the chemical exchange rate constant were obtained (Figs 3 and 4).

An attempt to evaluate the activation barrier by the full line shape analysis of the signal CH_2-4,7 was not successful because Arrhenius dependence of ln(k/T) *versus* 1/T was nonlinear (Fig. 4b).

Generally, two major factors lead to deviations from linearity in coordinates ln(k/T) *versus* 1/T: changing in the activity of the solute

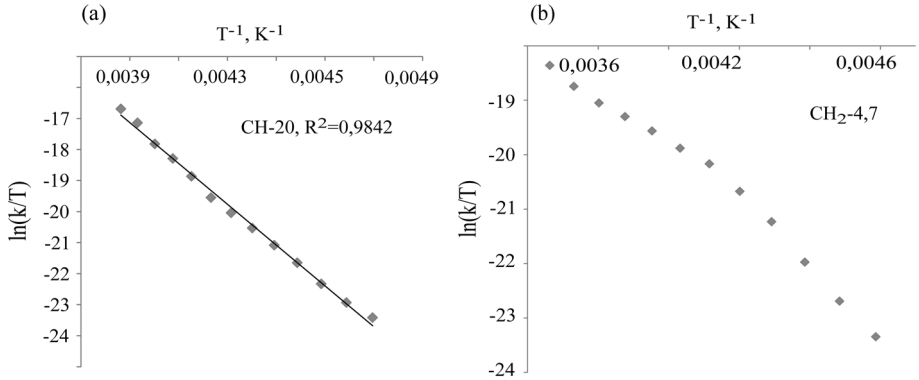

Figure 4. Arrhenius dependencies for compound I: (a) correspond to CH-20 group and (b) correspond to CH_2-4,7.

due to intermolecular interactions and connecting at least one extra process. It can be concluded from the analysis of this dependence and line shape of the signals CH_2-4 and CH_2-7 in the NMR ^{1}H NMR spectra at low temperatures that two conformational processes have an influence on the line shape of these signals. The first process is a transformation of seven-membered cycle between enantiomeric *P*-twist and *M*-twist conformations.[9,11] The second process is associated with a rotation of dinitrophenyl fragment around the C–O bond leading to conformational enantiomers due to the axial chirality (Fig. 5).[9,11,21–24] A similar phenomenon of axial chirality of conformers of seven-membered sulfur-containing twist forms of spirobisdithiepins was reported (Fig. 5) by Wade *et al.*[25]

Decelerating of one process leads to formation of two conformational enantiomers due to the helical element of chirality. When both processes are 'frozen out,' two pairs of conformational diastereomers can be seen in the NMR spectrum as two sets of signals for each functional group.

These conformational exchange effects are expressed differently on various signals due to the differences in the locations of proton groups. For example, the rotation process around the C–O bond has a greater impact into the line shape changes of CH-20 and CH_3-13 signals, while the process of transformation of seven-membered cycle mostly affects on the CH_2-4,7 and CH_3-8 resonance signals.

With the decreasing temperature, a typical spectroscopic picture for the ketals is observed; primarily, two AB quartets are partially 'frozen out' because of the conformational enantiotopomerization process. Then slowing down of second process on the NMR time scale leads to a diastereotopomerization and, as a result, to a doubling of the signal set.

An analysis of the dependence of the exchange rate constant from the temperature for the CH_2-4,7 signals was carried out using Origin 7.5 software (OriginLab Corporation)[20] by mathematical decomposition of the complex two-component exponential dependence into two simple one-component dependencies by the equation:

$$\frac{k}{T}=\frac{k_1}{T}+\frac{k_2}{T}=\frac{k_B}{h}*\exp\left(-\frac{\Delta G_1^{\ddagger}}{RT}\right)+\frac{k_B}{h}*\exp\left(-\frac{\Delta G_2^{\ddagger}}{RT}\right)$$

where k_1 and k_2 are the rate constants of two conformational exchange processes.

Thus, the energy barriers for each single one-component process were determined separately. Energy barriers of the conformational exchange are shown in Table 2. Calculated activation parameters are in good agreement with the parameters estimated using the coalescence temperature (Table 2).

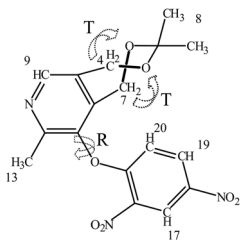

Figure 5. Intramolecular dynamic processes for compounds I and II (illustrated by I): rotation of dinitrophenyl fragment around the C–O bond (R) and twist–twist conformational transitions of the seven-membered cycle (T).

Dynamic ^{1}H NMR study of 9-(2,4-dinitrophenyloxy)-3,8-dimethyl-3-pentyl-1,5-dihydro-[1,3]dioxepino[5,6-c]pyridine

Compound II has an asymmetric ketal carbon atom that significantly influences the NMR spectrum compared with compound I.

Assignment of the signals of compound II in the ^{1}H NMR spectrum (Fig. 6) was made similarly to compound I and on the basis of 2D ^{1}H–^{1}H COSY spectra. In the ^{1}H NMR spectrum of compound II (Fig. 6) at the temperature of 303 K, the signals of methyl protons CH_3-8 and CH_3-25 are observed at $\delta = 1.38$ and $\delta = 0.89$ ppm, respectively. The CH_3-8 signal was observed at higher frequency than the CH_3-25 because of neighboring electronegative oxygen atom (Figs 6 and 7).

As the temperature was decreasing, line shapes of the signals in ^{1}H NMR spectrum of compound II were changed (Fig. 7a). The

Table 2. Activation parameters of the conformational exchange for compound I

^{1}H NMR signals	T_c, K	$\Delta G^{\ddagger}_{203}$ (kcal/mol)	
		Calculated from the coalescence temperature (kcal/mol)	Calculated from the line shape analysis (kcal/mol)
CH-20	227	10.1 (R)	9.9 (R)
CH_3-13	217	9.7 (R)	9.6 (R)
CH_2-4,7	210, 263	10.3 (R); 12.0 (T)	10.2 (R); 12.5 (T)

R, rotation of the dinitrophenyl fragment around the C–O bond; T, twist–twist variation of the geometry of the seven-membered cycle.

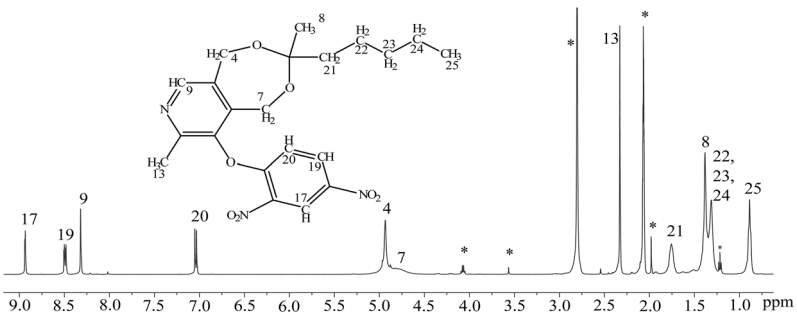

Figure 6. Molecular structure and ^{1}H NMR spectra of compound II dissolved in acetone-d_6 at 303 K. The solvent signal is marked by an asterisk.

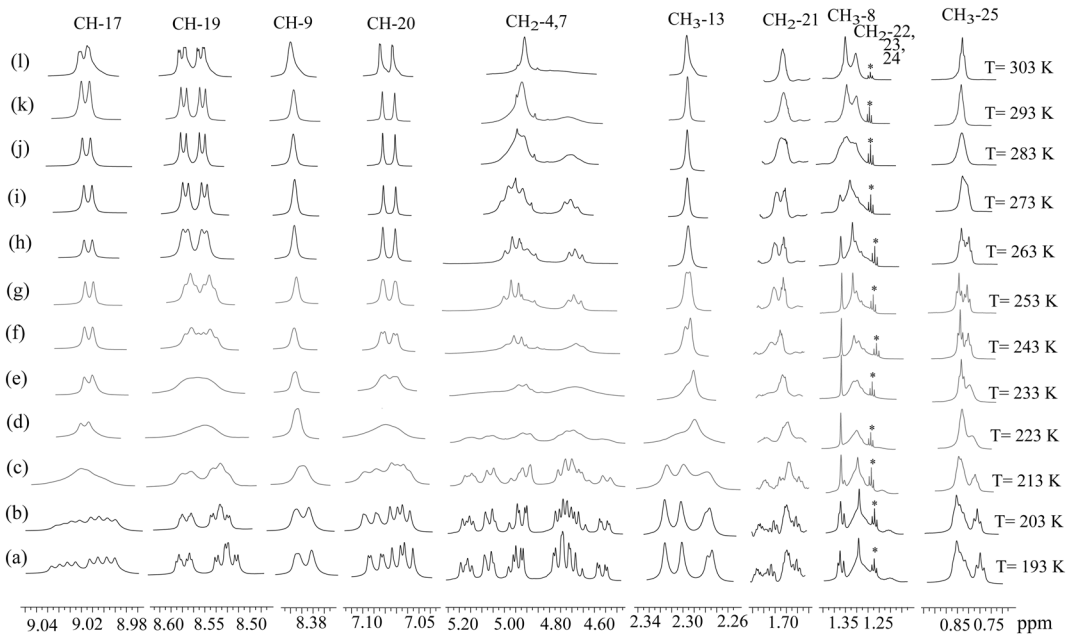

Figure 7. ^{1}H NMR spectra of compound II in acetone-d_6 solution at different temperatures. The signals of the solvent and impurities are marked by asterisks.

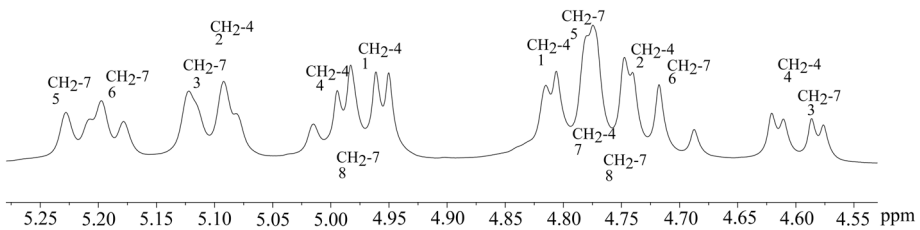

Figure 8. Partial ^{1}H NMR spectra containing the signals of methylene groups of compound II in acetone-d_6 solution. The numbering denotes the assignment of signal components to AB quadruplets: 1, 2, 4, and 7 for CH_2-4 and 3, 5, 6, and 8 for CH_2-7.

CH_2-4 signal was broadened and split into two groups of signals with temperature lowering, while the CH_2-7 signal was first narrowed, then broadened, and finally split into two groups of signals. Finally, at the temperature of 193 K, these protons were presented in the NMR spectrum as eight AB quartets (Figs 7 and 8). The proton signals CH-20 and CH-13 in the spectrum at the low temperature were presented as four doublets and four singlets, respectively. Thus, the number of these signals was fourfold increase compared with the spectrum at room temperature (Table 3; Figs 8 and 9).

The integral intensity of the signals belonging to different forms allowed us to determine the content ratio of the different conformations, which were approximately related as 1.52.1.52.1.1. The energy barriers of the conformational exchange were calculated using a line shape analysis (Fig. 9) and are shown in Table 4.

As one can see from Table 4, compound II also takes part in two similar conformational exchange processes as compound I. The energy barrier for a process of rotation of dinitrophenyl fragment around C–O bond for compound II is almost the same as it was for compound I. However, the activation energy for the second conformational exchange process caused by transformation of seven-membered cycle conformation between enantiomeric *P*-conformation and *M*-conformation of the helical type (twist) is different. The larger $\Delta G^{\neq}_{203}$-value of compound II is explained by

Table 3. ^{1}H NMR spectra parameters (δ, ppm) and spin-spin interaction constants (J, Hz) for compound II in acetone-d_6 at different temperatures [a]

T, K	CH-9	CH_2-4; CH_2-7	CH_3-8	CH_3-13	CH_2-22,23,24	CH_3-25	CH-20; CH-19; CH-17
293	8.33	4.94; 4.73*	1.38	2.33	1.75*	0.88	7.04, 7.06 (9.3); 8.49, 8.51 (9.3, 2.8); 8.95 (2.8)
273	8.34	4.95*; 4.71*	1.40	2.32	1.71*, 1.77*	0.87*	7.04, 7.06 (9.3); 8.50 (9.3, 2.8); 8.96 (2.8)
243	8.36	4.97; 4.74, 5.12	1.39	2.31	1.56–1.81*	0.87	7.06*; 8.52*; 8.99
223	8.37	4.96*, 4.77, 5.12 (14.9); 4.60, 4.69, 5.19, 5.21 (17.1)	1.38, 1.36	2.31, 2.33, 2.28	1.54–1.92*	0.78*, 0.86*	7.04*, 7.06*, 7.08*, 7.10*; 8.50*, 8.56; 9.00*
193	8.37, 8.38*	4.95, 4.97, 4.78, 4.75, 4.58, 4.74, 5.08, 5.01, (16.5); 5.07, 5.08, 4.71, 4,73, 4.57, 4.68, 5.19, 5.23 (15.5)	1.35, 1.37, 1.37, 1.38	2.30, 2.33, 2.27, 2.27	1.51–1.93*	0.76, 0.84*	7.04, 7.06 (9.3), 7.09, 7.09 (9.3); 8.49, 8.51, 8.57, 8.58 (9.3, 2.8); 8.99, 9.00, 9.02, 9.03 (2.8)

[a]Notation: chemical shifts of dominant form signals are underlined.
* This means broadened signal.

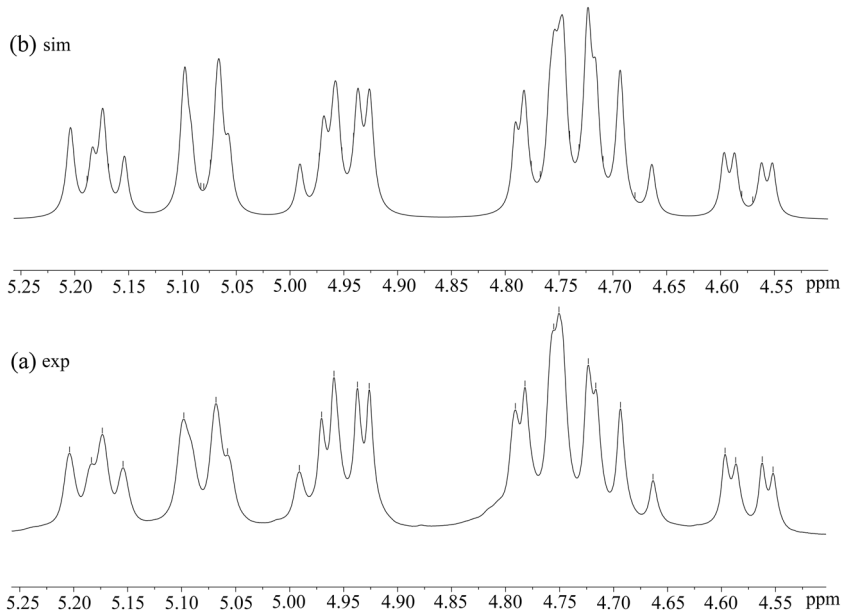

Figure 9. (a) Partial experimental ^{1}H NMR spectrum containing the signals of the methylene groups and (b) simulation in MestReNova program.

Table 4. Activation parameters of the conformational exchange for compound II

^{1}H NMR signals	T_c, K	$\Delta G^{\neq}_{203}$ (kcal/mol)	
		Calculated from the coalescence temperature (kcal/mol)	Calculated from the line shape analysis (kcal/mol)
CH-20	213, 243	10.7 (R); 13.8 (T)	10.8 (R)
CH-17	213	10.9 (R)	10.6 (R)
CH_3-13	223, 263	10.6 (R); 14.3 (T)	—
CH-9	213	11.2 (R)	10.2 (R); 13.9 (T)
CH_2-4,7	233, 300	10.5 (R); 14.1 (T)	—

R, rotation of the dinitrophenyl fragment around the C–O bond; T, twist–twist variation of the geometry of the seven-membered cycle.

a sterically larger substituent in seven-membered ring, which hampers conformational transitions of the cycle.

Semiempirical calculations of the rotational barriers

PM3 calculations of rotational barriers were carried out using the HyperChem 8 (Hypercube, Inc., Gainesville, FL, USA) software in order to define which activation barrier corresponds the rotation 2,4-dintrophenyl moiety. Computations revealed that the rotations around the C2–O3 and O3–C10 bonds are strongly synchronized for both compounds and should be calculated together. During the calculations, the values of torsion angles φ_1(C1,C2,O3,C10) and φ_2(C2,O3,C10,C11) (Fig. 1) were changed independently in steps of 10°, and full geometry optimization was carried out at each point. The resulting potential energy surfaces are shown in Figs 10 and 11.

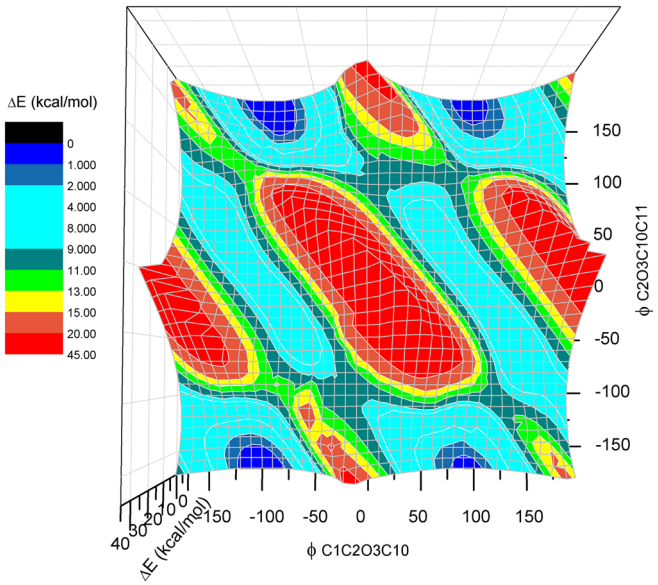

Figure 10. Potential energy surface of the dinitrophenyl fragment rotation around C1–O3 and O3–C10 bonds for compound I.

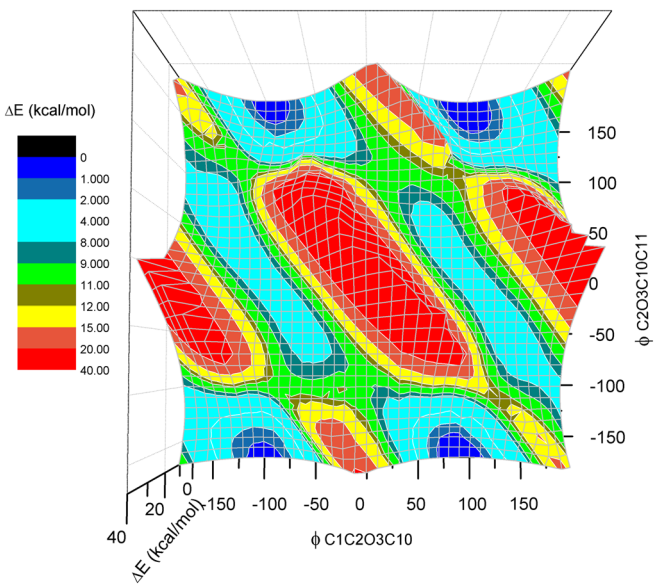

Figure 11. Potential energy surface of the dinitrophenyl fragment rotation around C1–O3 and O3–C10 bonds for compound II.

Table 5. Calculated energy barriers of the dinitrophenyl fragment rotation around the C–O bond for compounds I and II

Compound I			Compound II		
φ_1 (°)	φ_2 (°)	ΔE (kcal/mol)	φ_1 (°)	φ_2 (°)	ΔE (kcal/mol)
−120	110	12.0	−120	110	10.2
80	100	11.0	80	100	11.4
−80	−100	10.8	−80	−100	10.7
120	−110	10.3	120	−110	11.9

As it can be seen from Figs 10 and 11, the rotation of 2,4-dintrophenyl moiety is similar for both compounds I and II and leads to two rotational conformations at $\varphi_1 = 100°/\varphi_2 = 180°$ and $\varphi_1 = -100°/\varphi_2 = 180°$. Calculated rotational barriers (Table 5) are in good agreement with dynamic NMR data for the first conformational process and confirm that the rotation of dinitrophenyl group decelerates at lower temperatures than the transformation of the seven-membered ketal ring (Table 5).

Conclusions

Conformational features and dynamic processes for dinitrophenyloxy derivatives of seven-membered cyclic ketals of pyridoxine were studied by dynamic NMR experiments. These compounds are involved in two conformational exchange processes. One process is the rotation of the dinitrophenyl fragment around the C–O bond, and the second process is a conformational transformation of the seven-membered cycle. Activation barriers of both conformational exchange processes were determined using line shape analysis of the NMR spectra with variation of temperature. It was shown that the energy barriers of the dinitrophenyl fragment rotation around the C–O bond are almost the same for both compounds studied. However, activation energy of the second conformational exchange process caused by the transformation of the seven-membered cycle conformation strongly depends on the type of substituent in the cycle. According to the computational data, the rotation of the dinitrophenyl group corresponds to the lower activation barrier.

Acknowledgements

This work was funded by the subsidy allocated to Kazan Federal University for the project part of the state assignment in the sphere of scientific activities. The work was also performed according to the Russian Government Program of Competitive Growth of Kazan Federal University.

References

[1] B. A. Arbuzov, V. V. Klochkov, A. V. Aganov, E. N. Klimoviiskii, U. U. Samitov. *Dokl. Akad. Nauk SSSR* **1980**, 250, 378–381.
[2] B. A. Arbuzov, E. N. Klimovitskii, A. B. Remizov, V. V. Klochkov, A. V. Aganov, M. B. Timirbaev. *Russ. Chem. Bull.* **1980**, *29*, 8, 1276–1281.
[3] O. V. Aganova, L. F. Galiullina, A. V. Aganov, Y. G. Shtyrlin, M. V. Pugachev, N. V. Shtyrlin, V. V. Klochkov. *Appl. Magn. Reson.* **2014**, *45*(7), 653–665.
[4] a) E. N. Klimovitski, D. Y. Strelnik, V. V. Klochkov, S. K. Latypov. *Zh. Org. Khim.* **1992**, *28*(8), 1587–1596; b) E. N. Klimovitskii, G. N. Sergeeva, K. A. Ilyasov, S. K. Latypov, V. V. Klochkov, R. K. Almyanova, B. A. Arbuzov. *Zh. Obshch. Khim.* **1987**, *57* 10, 2207–2215.
[5] a) B. A. Arbuzov, E. N. Klimovitskii, A. B. Remizov, M. B. Timirbaev. *Zh. Obshch. Khim.* **1981**, *51*(12), 2705–2710; b) V. V. Klochkov, S. K. Latypov, A. V. Aganov. *Zh. Obshch. Khim.* **1993**, *63* 4, 721–739.
[6] E. N. Klimovitskii, Y. G. Shtyrlin, E. A. Kashaeva, V. D. Kiselev, R. M. Vafina, A. V. Khotinen. *Zh. Obshch. Khim.* **1996**, *66*(3), 491–498.
[7] Y. G. Shtyrlin, V. Y. Fedorenko, E. N. Klimovitskii. *Zh. Obshch. Khim* **2001**, *71*(5), 819–820.
[8] Y. G. Shtyrlin, G. R. Shaikhutdinova, E. N. Klimovitskii. *Zh. Obshch. Khim.* **2001**, *71*(3), 464–468.
[9] I. Z. Rakhmatullin, L. F. Galiullina, M. R. Garipov, A. D. Strel'nik, Y. G. Shtyrlin, V. V. Klochkov. *Magn. Reson. Chem.* **2014**, *52*(12), 769–778.
[10] A. D. Strel'nik, M. R. Garipov, A. S. Petukhov, N. V. Shtyrlin, O. A. Lodochnikova, I. A. Litvinov, A. K. Naumov, O. A. Morozov, A. E. Klimovitskii, Y. G. Shtyrlin. *Spectrochim. Acta A Mol. Biomol. Spectrosc.* **2014**, *117*(3), 793–797.

[11] A. S. Petukhov, A. D. Strel'nik, V. Y. Fedorenko, I. A. Litvinov, O. A. Lodochnikova, Y. G. Shtyrlin, E. N. Klimovitskii. *Russ. J. Gen. Chem.* **2007**, *77*, 1416–1421.
[12] Y. G. Shtyrlin, O. A. Morozov, I. A. Litvinov, O. A. Lodochnikova, N. V. Shtyrlin, M. R. Garipov, A. S. Petukhov, A. V. Lovchev, A. S. Strel'nik. Pat. RU2501801, MPC C07D491/056, 20.12. **2003**.
[13] H. J. Reich, University of Wisconsin, WINDNMR-Pro, a windows program for simulating high-resolution NMR spectra. http://www.chem.wisc.edu/areas/reich/plt/windnmr.htm, 11. 02. **2002**.
[14] N. M. Sergeev. *Usp. Khim.* **1973**, *42*(5), 789–798.
[15] F. H. Karataeva, V. V. Klochkov, *^{1}H and ^{13}C NMR Spectroscopy in Organic Chemistry*, Kazan State University, Kazan, **2007**.
[16] S. Benson, *Fundamentals of Chemical Kinetics*, Mir, Moscow, **1964**.
[17] N. M. Emanuel, D. G. Knorre, *Course of Chemical Kinetics*, Vyshaya shcola, Moscow, **1984**.
[18] S. G. Entelis, R. P. Tiger, *The Kinetics of Reactions in the Liquid Phase. Quantitative Account of the Influence of the Environment*, Khimiya, Moscow, **1973**.
[19] D. Casarini, L. Lunazzi, A. Mazzanti. *Eur. Org. Chem.* **2010**, *11*, 2035–2056.
[20] H. Stone. *J. Opt. Soc. Am.* **1992**, *52*(9), 998–1003.
[21] D. Casarini, E. Foresti, F. Gasparrini, L. Lunazzi, D. Macciantelli, D. Misiti, C. Villani. *J. Org. Chem.* **1993**, *58*, 5674–5682.
[22] C. Daniele, L. Lunazzi. *J. Org. Chem.* **1995**, *60*, 97–102.
[23] D. Casarini, L. Lunazzi, A. Mazzanti. *J. Org. Chem.* **1997**, *62*, 3315–3323.
[24] D. Casarini, L. Lunazzi, A. Mazzanti. *J. Org. Chem.* **1997**, *62*, 7592–7596.
[25] E. O. Wade, R. A. Valiulin, L. A. Ruybal, A. G. Kutateladze. *Org. Lett.* **2006**, *8*(22), 5121–5124.